J|A|C|S COMMUNICATIONS

Published on Web 10/08/2010

Simple Combustion Production and Characterization of Octahydro[60]fullerene with a Non-IPR C_{60} Cage

Qun-Hong Weng,[†] Qiao He,[†] Ting Liu,[†] Hui-Ying Huang,[‡] Jian-Hua Chen,[†] Zhi-Yong Gao,[†] Su-Yuan Xie,*[,†] Xin Lu,*[,†] Rong-Bin Huang,[†] and Lan-Sun Zheng[†]

State Key Laboratory of Physical Chemistry of Solid Surface, and Department of Chemistry, College of Chemistry and Chemical Engineering and School of Life Science, Xiamen University, Xiamen, 361005, China

Received April 15, 2010; E-mail: xinlu@xmu.edu.cn (X.L.); syxie@xmu.edu.cn (S.Y.X.)

Abstract: For the first time an easier, operable combustion method is employed for the synthesis of non-IPR fullerene, and an octahydro[60]fullerene with a non-IPR C_{60} cage (C_{60} isomer $^{\#1809}C_{60}$) produced by combustion is isolated and characterized by MS, UV−vis, IR, and NMR spectroscopies in combination with DFT calculations. This finding shows that, in addition to chlorine, hydrogen can be an ample cataloreactant for the production of non-IPR fullerene derivatives under such conditions as arc-burning and diffusion combustion.

Fullerenes violating the isolated pentagon rule (IPR)[1] have caught much attention[2] ever since discovery of the first buckyball molecule C_{60},[3] which itself is the smallest IPR-satisfying fullerene. It was believed that non-IPR fullerenes with abutting pentagons play a pivotal role (e.g., as precursors) in the formation of stable IPR-satisfying fullerenes.[4,5] However, the inherent instability of non-IPR fullerenes pertaining to their abutting pentagons[6] poses difficulties in the synthesis, isolation, and chemical manipulation of pristine non-IPR fullerenes. Nevertheless, recent experimental and theoretical investigations have shown that non-IPR fullerenes can be effectively stabilized by endohedral encapsulation or exohedral functionalization.[2] An increasing number of non-IPR fullerenes have been synthesized and characterized as endohedral fullerenes, e.g., $Sc_3N@C_{68}$[7] and $Sc_2C_2@C_{68}$,[8] and exohedral derivatives including $C_{50}Cl_{10}$,[9] $C_{58}F_{18}$,[10] $C_{64}X_4$ (X = H[11] and Cl[9b]), $C_{56}Cl_{10}$,[12] $C_{60}Cl_n$ (n = 8,12),[13] $C_{76}Cl_{24}$,[14] $C_{54}Cl_8$, $C_{56}Cl_{12}$, $C_{66}Cl_6$, and $C_{66}Cl_{10}$.[15] Most of these non-IPR fullerene derivatives were produced by means of graphite arc-discharge. It should be noted that in the macroscopic production of fullerenes, graphite arc-discharge is far less efficient than the combustion method. The latter's merits are easier operable synthetic device, higher yield of fullerene soot, and consecutive synthesis.[16,17] It is stimulating that we recently detected in combustion-produced soot the presence of $C_{64}H_4$,[17c] which likely has a non-IPR fullerene cage.[11] Herein we report the production of a new hydro[60]fullerene $C_{60}H_8$ with a non-IPR cage (C_{60} isomer #1809 termed by the spiral algorithm[18]) by the simple combustion method. The structure of this novel fullride has been characterized by MS, UV/vis, IR, and NMR spectroscopies in combination with density functional theory (DFT) calculations.

Soot containing $C_{60}H_8$ was produced by a modified diffusion combustion approach,[19] in which the mixtures of acetylene and benzene with oxygen were burnt at 15−20 Torr in a steel chamber. The optimized gas flow rates are 0.55 L/min for O_2, 1.10 L/min for C_2H_2, and 1.0−1.1 L/min for vaporous benzene. During the process of combustion, hot flow of the gaseous products from the chamber carried soot through a water-cooled conduit onto a filter paper, just outside the combustion furnace for gathering the soot. The soot productivity can be up to 5 g per hour efficiently.

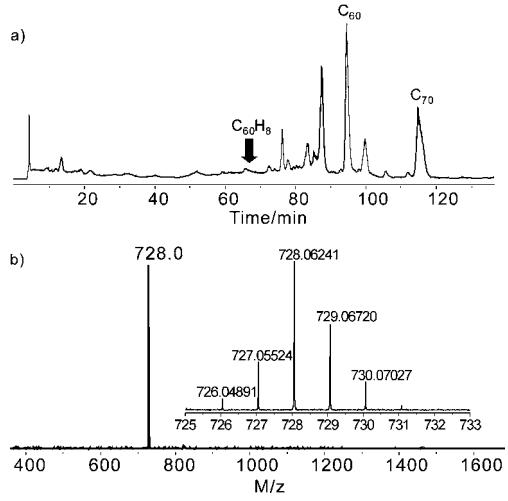

Figure 1. (a) HPLC/APCI-MS chromatogram of toluene-extracted soot products. (b) APCI-MS for $C_{60}H_8$ with isotope distribution (high-resolution MS) inset.

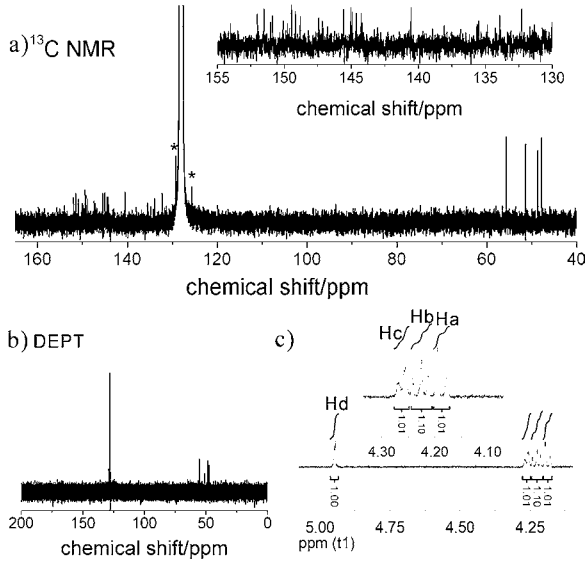

Figure 2. (a) ^{13}C NMR spectrum of $C_{60}H_8$ (150 MHz, C_6D_6 solvent, room temperature). The asterisk-marked signals are due to residual toluene. (b) DEPT spectrum. (c) ^{1}H NMR spectrum (600 MHz, C_6D_6 solvent, room temperature).

[†] State Key Laboratory of Physical Chemistry of Solid Surface.
[‡] School of Life Science.

Separation of $C_{60}H_8$ from the trapped soot was conducted using a high pressure liquid chromatography (HPLC) (see Supporting Information for the synthetic device and HPLC isolation of $C_{60}H_8$). Figure 1a shows the HPLC/mass spectra of a prepurified extract solution from the combustion soot; the major products are C_{60} and C_{70} with $C_{60}H_8$ as a minor component. An amount of ~5 mg $C_{60}H_8$ with purity up to 99% was finally isolated and characterized by means of UV/vis, IR, and NMR spectroscopies. The high-resolution mass spectrum (Figure 1b) of purified $C_{60}H_8$ sample shows the molecular ion peak of 728 amu, agreeing well with the simulated mass spectrum of $C_{60}H_8$.

Solution of $C_{60}H_8$ in cyclohexane or benzene is light yellow. The ^{13}C NMR spectrum of $C_{60}H_8$ in C_6D_6 solvent (Figure 2a) shows four upfield signals (4 × 2, 47.8, 48.7, 51.3, and 55.7 ppm) arising from sp^3-hybridized carbon atoms, and about 27 downfield signals ranging from 132.3 ppm to 152.0 ppm pertaining to sp^2-hybridized carbon atoms. DEPT spectrum (Figure 2b) further indicates that $C_{60}H_8$ has in total four types of sp^3-hybridized carbon atoms attached by H atoms, suggesting this molecule belongs to C_s, C_2, or C_i point group of symmetry.

The ^1H NMR spectrum of $C_{60}H_8$ in C_6D_6 solvent (Figure 2c) comprises four parts (H_a, H_b, H_c, and H_d) with the peak-area integral ratio 2:2:2:2. The doublet peak at 4.95 ppm (H_d) is clearly discerned from the multiplet peaks around 4.2 ppm for H_a, H_b, and H_c. With the aid of 2D $^1H-^1H$ COSY spectrum (Figure 3), the multiplet peaks could be disassembled clearly: H_a (doublet, 4.19 ppm, 2H), H_b (triplet, 4.22 ppm, 2H) and H_c (quadruplet, 4.26 ppm, 2H). The COSY spectrum also indicates the following spin−spin coupling correlations. First, H_d is weakly correlated to H_c with a coupling constant (J_{cd}) of 2.4 Hz. Second, H_a is strongly correlated to H_b (J_{ab} = 10.3 Hz). Third, H_b is strongly correlated to H_a and H_c. Based on J_{ab} and J_{cd}, the coupling constant J_{bc} for the spin−spin coupling between H_b and H_c is estimated to be ~7.0 Hz. Thus, the $C_{60}H_8$ has four types of H atoms; among them, H_a, H_b, and H_c are linked to three sequentially neighboring carbon atoms, whereas the H_d-linked carbon atom is by one or two sp^2-hybridized carbon atoms away from the H_c-linked carbon atom.

Yet, the aforementioned NMR spectra are not enough to afford a clear-cut determination of the $C_{60}H_8$ structure. On account of the harsh synthetic conditions, final products surviving from the combustion process are likely thermodynamically favored. Hence, we performed semiempirical PM3[20] calculations and DFT calculations at the PBE/DNP level of theory[21] to search for the lowest-energy structure of $C_{60}H_8$, in which the C_{60} cage may be the IPR-satisfying one, i.e., $^{\#1812}C_{60}$,[18,22] or a non-IPR one, e.g., $^{\#1809}C_{60}$.[13] Figure 4 shows three low-energy isomers of $C_{60}H_8$ from PBE/DNP calculations. Both isomers **1** and **2** contain the same non-IPR $^{\#1809}C_{60}$ cage with two pentagon−pentagon fusions, while isomer **3** has the $^{\#1812}C_{60}$ cage. Among them, the C_s-symmetric isomer **1** is the lowest-energy isomer of $C_{60}H_8$; isomer **2**, isostructural to the previously synthesized $^{\#1809}C_{60}Cl_8$,[13] is by 4.6 kcal mol^{-1} less stable than **1**; isomer **3** is by 15.8 kcal mol^{-1} higher in energy than **1**. Noteworthily, the lowest-energy isomer **1** has the structural features (symmetry and H positions) deduced from the NMR spectra.

We then computed the NMR chemical shifts and $^1H-^1H$ spin−spin coupling constants of $C_{60}H_8$ **1** at the GIAO-B3LYP/6-31G** level of theory.[23] The DFT-predicted $^1H-^1H$ spin−spin coupling constants (J_{ab} ≈ 10.5, J_{bc} ≈ 7.5, J_{cd} ≈ 4.2 Hz) agree well with the experimental ones (J_{ab} ≈ 10.3, J_{bc} ≈ 7.0, J_{cd} ≈ 2.4 Hz). The predicted ^1H chemical shifts for the four types of H atoms (H_a ≈ 4.7, H_b ≈ 4.5, H_c ≈ 4.7, and H_d ≈ 5.4 ppm) are comparable to the experimental ones (4.2, 4.2, 4.3, 4.9 ppm). For the four types of sp^3-hybridized carbon atoms, the DFT-calculated ^{13}C chemical shifts are 52.9 (C_a), 52.5(C_b), 55.7 (C_c), and 59.4 (C_d) ppm, corresponding to the measured ones, 48.7, 47.8, 51.3, and 55.7 ppm.[24] The computed ^{13}C chemical shifts for 27 types of sp^2-hybridized carbon atoms (25 × 2, 2 × 1) range from 132.1 to 150.7 ppm, in accordance with the measured ones ranging from 132.3 to 152.0 ppm (see Supporting Information for details). These computational data clearly show that the synthesized $C_{60}H_8$ is isomer **1** with a non-IPR C_{60} cage.

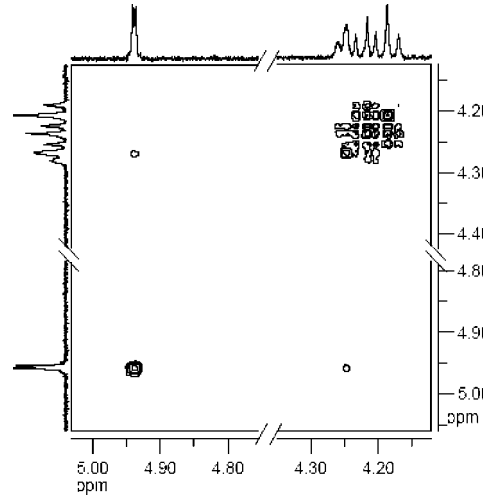

Figure 3. Selected range of $^1H-^1H$ COSY spectrum of $C_{60}H_8$.

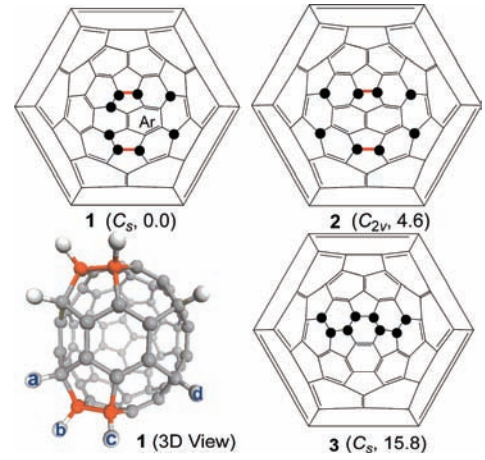

Figure 4. Schlegel diagrams (black dots: H-linked C atoms) for three low-energy isomers **1**−**3** of $C_{60}H_8$, together with the ball-and-stick model of the lowest-energy isomer **1**. PBE/DNP-predicted symmetry and relative energy (in kcal mol^{-1}) are given in parentheses.

The IR spectrum of $C_{60}H_8$ (Supporting Information) shows intense absorptions around 2900 cm^{-1}, a fingerprint of tertiary CH moieties.[25] The UV/vis spectrum (Supporting Information) of $C_{60}H_8$ in cyclohexane solution shows absorptions at 215, 254, 280, 342, and 393 nm, differing slightly from those of $^{\#1812}C_{60}$ (absorptions at 210, 256, 328, 405 nm).[13] The PBE/DNP-predicted HOMO−LUMO gap of $^{\#1809}C_{60}H_8$ **1** is 1.67 eV, equal to that of $^{\#1812}C_{60}$. Both UV/vis spectrum and DFT calculations show $^{\#1809}C_{60}H_8$ is a wide band gap fulleride.

It is interesting to note that the newly synthesized $^{\#1809}C_{60}H_8$ isomer **1** (Figure 4) differs in structure from the previously reported $^{\#1809}C_{60}Cl_8$ isomer **2**, despite both compounds sharing the same non-IPR $^{\#1809}C_{60}$ cage and having the same number of exohedral addends. In accordance with such experimental observations, PBE/DNP computations revealed that for the octa-chlorinated case $^{\#1809}C_{60}Cl_8$ **2** is by 3.0 kcal mol^{-1} more stable than $^{\#1809}C_{60}Cl_8$ **1**,

while for the octa-hydrogenated case, $^{\#1809}C_{60}H_8$ **1** is by 4.6 kcal mol^{-1} more stable than isomer **2**. Thus, the exohedral addition pattern of $^{\#1809}C_{60}$ depends on the nature of addends. A similar trend could be found for the different hydrogenation/chlorination patterns of $^{\#1812}C_{60}$.[26] That is, chlorine atoms are more spatial and more sterically repulsive than hydrogen atoms, and as a result, addends tend to lie together in $C_{60}H_n$ and to be separated apart in $C_{60}Cl_n$.[26]

Note that $^{\#1809}C_{60}H_8$ isomer **1** and $^{\#1809}C_{60}Cl_8$ isomer **2** share the common features that the active pentagon−pentagon fusions of the non-IPR carbon cage are completely saturated by H or Cl atoms and their small sp^2-hybridized carbon fragments, i.e. a benzene-like C_6 ring in $^{\#1809}C_{60}H_8$ **1** and a naphthalene-like C_{10} ring in $^{\#1809}C_{60}Cl_8$ isomer **2**, fulfill the Hückel rule of aromaticity. These two special addition patterns of H/Cl addends improve the planarity of the sp^2-hybridized carbon fragments and, hence, enhance their π-electronic conjugation and delocalization.[27] These features account for the stability of both non-IPR $^{\#1809}C_{60}$ derivatives. In addition, the very small energy gap between isomers **1** and **2** for both the chlorinated and hydrogenated cases suggests that $^{\#1809}C_{60}H_8$ isomer **2** and $^{\#1809}C_{60}Cl_8$ isomer **1** also could be synthetically viable and deserve further experiments.[28]

In conclusion, we have synthesized a non-IPR fullerene derivative by simple combustion of gaseous acetylene/benzene mixture. The synthesized crown-shaped octahydro[60]fullerene, though sharing the same non-IPR $^{\#1809}C_{60}$ cage with $^{\#1809}C_{60}Cl_8$,[13] is the first hydrogenated fulleride of non-IPR C_{60}. Moreover, the successful synthesis of this non-IPR hydro[60]fullerene shows that in addition to chlorine, hydrogen can be an ample cataloreactant for the production of non-IPR fullerene derivatives under such conditions as arc-burning and combustion. Further experiments are in progress in our laboratory to synthesize other non-IPR fullerenes by the hydrogen-involving arc-burning and combustion processes.

Acknowledgment. This work was sponsored by NSFC (Nos. 20525103, 20673088, 20973137, 20721001, 20423002, 21031004) and 973 projects (Nos. 2007CB815301 and 2007CB815307).

Supporting Information Available: Scheme of synthesis apparatus, chromatograms of isolation of $C_{60}H_8$, IR and UV/vis spectra of $C_{60}H_8$, thermostability of $C_{60}H_8$, PM3- and PBE/DNP-computed relative energies of $C_{60}H_8$ isomers, details of GIAO-B3LYP NMR calculations of $C_{60}H_8$, Cartesian coordinates of $C_{60}H_8$ isomers, and complete ref 23d. This material is available free of charge via the Internet at http://pubs.acs.org.

References

(1) Kroto, H. W. *Nature* **1987**, *329*, 529.
(2) Tan, Y. Z.; Xie, S. Y.; Huang, R. B.; Zheng, L. S. *Nat. Chem.* **2009**, *1*, 450–460.
(3) Kroto, H. W.; Heath, J. R.; O'Brien, S. C.; Curl, R. F.; Smalley, R. E. *Nature* **1985**, *318*, 162.
(4) (a) Smalley, R. E. *Acc. Chem. Res.* **1992**, *25*, 98. (b) Heath, J. R. *ACS Symp. Ser.* **1991**, *24*, 1. (c) McElvany, S. W.; Ross, M. M.; Goroff, N. S.; Diederich, F. *Science* **1993**, *259*, 1594.
(5) Kietzmann, H.; Rochow, R.; Ganteför, G.; Eberhardt, W.; Vietze, K.; Seifert, G.; Fowler, P. W. *Phys. Rev. Lett.* **1998**, *81*, 5378.
(6) Lu, X.; Chen, Z. *Chem. Rev.* **2005**, *105*, 3643, and references therein.
(7) Stevenson, S.; Fowler, P. W.; Heine, T.; Duchamp, J. C.; Rice, G.; Glass, T.; Harich, K.; Hajdu, E.; Bible, R.; Dorn, H. C. *Nature* **2000**, *408*, 427.
(8) Shi, Z. Q.; Wu, X.; Wang, C. R.; Lu, X.; Shinohara, H. *Angew. Chem., Int. Ed.* **2006**, *45*, 2107.
(9) (a) Xie, S. Y.; Gao, F.; Lu, X.; Huang, R. B.; Wang, C. R.; Zhang, X.; Liu, M. L.; Deng, S. L.; Zheng, L. S. *Science* **2004**, *304*, 699. (b) Han, X.; Zhou, S. J.; Tan, Y. Z.; Wu, X.; Gao, F.; Liao, Z. J.; Huang, R. B.; Feng, Y. Q.; Lu, X.; Xie, S. Y.; Zheng, L. S. *Angew. Chem., Int. Ed.* **2008**, *47*, 5340.
(10) Troshin, P. A.; Avent, A. G.; Darwish, A. D.; Martsinovich, N.; Abdul-Sada, A. K.; Street, J. M.; Taylor, R. *Science* **2005**, *309*, 278.
(11) Wang, C. R.; Shi, Z. Q.; Wan, L. J.; Lu, X.; Dunsch, L.; Shu, C. Y.; Tang, Y. L.; Shinohara, H. *J. Am. Chem. Soc.* **2006**, *128*, 6605.
(12) Tan, Y. Z.; Han, X.; Wu, X.; Meng, Y. Y.; Zhu, F.; Qian, Z. Z.; Liao, Z. J.; Chen, M. H.; Lu, X.; Xie, S. Y.; Huang, R. B.; Zheng, L. S. *J. Am. Chem. Soc.* **2008**, *130*, 15240.
(13) Tan, Y. Z.; Liao, Z. J.; Qian, Z. Z.; Chen, R. T.; Wu, X.; Han, X.; Zhu, F.; Zhou, S. J.; Zheng, Z. P.; Lu, X.; Xie, S. Y.; Huang, R. B.; Zheng, L. S. *Nat. Mater.* **2008**, *7*, 790.
(14) Ioffe, I. N.; Goryunkov, A. A.; Tamm, N. B.; Sidorov, L. N.; Kemnitz, E.; Troyanov, S. I. *Angew. Chem., Int. Ed.* **2009**, *48*, 5904.
(15) Tan, Y.-Z.; Li, J.; Zhu, F.; Han, X.; Jiang, W.-S.; Huang, R.-B.; Zheng, Z.; Qian, Z.-Z.; Chen, R.-T.; Liao, Z.-J.; Xie, S.-Y.; Lu, X.; Zheng, L.-S. *Nat. Chem.* **2010**, *2*, 269–273.
(16) Howard, J. B.; McKinnon, J. T.; Makarovsky, Y.; Lafleur, A.; Johnson, M. E. *Nature*, **1991**, *352*, 139.
(17) (a) Gerhardt, P.; Löffler, S.; Homann, K. H. *Chem. Phys. Lett.* **1987**, *137*, 306. (b) Howard, J. B.; McKinnon, J. T.; Johnson, M. E.; Makarovsky, Y.; Lafleur, A. L. *J. Phys. Chem.* **1992**, *96*, 6657. (c) Gao, Z. Y.; Jiang, W. S.; Sun, D.; Xie, S. Y.; Huang, R. B.; Zheng, L. S. *Combust. Flame* **2010**, *157*, 966.
(18) Fowler, P. W.; Manoloupoulos, D. E. *An Atlas of Fullerenes*; Oxford University Press: Oxford, 1995.
(19) Weng, Q.-H.; Sun, D.; Lin, S.-C. CN patent 200,910,111,152.8, 2009.
(20) Stewart, J. J. P. *J. Comput. Chem.* **1989**, *10*, 209.
(21) DNP refers to double numerical basis sets plus polarization. For the PBE density functional, see: (a) Perdew, J. P.; Burke, K.; Ernzerhof, M. *Phys. Rev. Lett.* **1996**, *77*, 3865. The PBE/DNP calculations were performed with the Dmol3 code implemented in Material Studio 3.0, Accelrys Inc. (b) Delley, B. *J. Chem. Phys.* **1990**, *92*, 508. (c) Delley, B. *J. Chem. Phys.* **2000**, *113*, 7756.
(22) For examples of investigations on the relative stability of $C_{60}H_8$ isomers containing the IPR-satisfying I_h-C_{60} cage, see: (a) Van Lier, G.; De Proft, F.; Geerlings, P. *Phys. Solid State* **2002**, *44*, 560. (b) Choho, K.; Van Lier, G.; Van De Woude, G.; Geerlings, P. *J. Chem. Soc. Perkin Trans. 2* **1996**, 1723.
(23) For the hybrid density functional B3LYP method, see: (a) Becke, A. D. *J. Chem. Phys.* **1993**, *98*, 5648. (b) Lee, C.; Yang, W.; Parr, R. G. *Phys. Rev. B* **1988**, *37*, 785. For the GIAO method, see: (c) Wolinski, K.; Hilton, J. F.; Pulay, P. J. *J. Am. Chem. Soc.* **1990**, *112*, 8251, and references therein. The PM3 and GIAO-B3LYP calculations were performed with the Gaussian 09 A.02 suite of programs. (d) Frisch, M. J.; et al. *Gaussian09*, Rev. A.02; Gaussian, Inc.: Wallingford CT, 2009.
(24) The B3LYP-predicted chemical shifts of the sp^3-hybridized carbon are overestimated by ~4 ppm compared to the experimental data. This is also true for other hydrofullerenes such as C_{3v}-$C_{60}H_{18}$ and C_{3v}-$C_{64}H_4$. See the Supporting Information for details.
(25) Henderson, C. C.; Cahill, P. A. *Science* **1993**, *259*, 1885.
(26) Troyanov, S. I.; Kemnitz, E. *Eur. J. Org. Chem.* **2005**, 4951.
(27) Taylor, R. *Phys. Chem. Chem. Phys.* **2004**, *6*, 328.
(28) Zhou, T., Weng, Q. H., Xie, S. Y., Huang, R. B., Zheng, L. S. Unpublished results.

JA108316E